Int. J. Electrochem. Sci., 7 **(2012)** 5069 - 5083

International Journal of
ELECTROCHEMICAL
SCIENCE
www.electrochemsci.org

Electrochemical Detection of Hydrogen Peroxide Based on Graphene Oxide/Prussian Blue Modified Glassy Carbon Electrode

Abdullahi Mohamed Farah, Force Tefo Thema and Ezekiel Dixon Dikio[*]

Department of Chemistry, Vaal University of Technology, P. O. Box X021, Vanderbijlpark 1900, Republic of South Africa
[*]E-mail: ezekield@vut.ac.za

Received: 20 April 2012 / *Accepted:* 12 May 2012 / *Published:* 1 June 2012

Prussian blue (PB) and graphene oxide (GO) were synthesized and characterized by scanning electron microscopy (SEM) and Fourier transform infrared spectroscopy among others. The synthesized Prussian blue and graphene oxide were used in the modification of glass carbon electrodes for the chemical detection of hydrogen peroxide at pH 3, 5.12 and 7.4. Cyclic and square wave voltammetry of GC-PB and GC-GO-PB electrodes show significant cathodic and anodic detection of hydrogen peroxide predominantly at pH 5.12 and 7.4 indicating one electron transfer reaction at the electrode surface.

Keywords: Graphene oxide, Prussian blue, Hydrogen peroxide, Electrodes, Electron transfer

1. INTRODUCTION

Graphene, a two-dimensional single layer of graphite and one-atom-thick sheet material with interesting physical properties [1-2] has been considered as the mother of all graphitic structure. Graphene's unique structure, excellent electronic properties, thermal and chemical stability have shown great promise applications in the field of electronic nanodevices, energy-storage materials, transparent conducting electrodes, chemical and biological sensors [3-12]. These properties also make graphene a promising candidate for fundamental study of potential device applications such as field-effect transistors, gas sensors and electrochemical resonators [5].

Graphene is an ideal material for electrochemistry [13] because of its very large 2D electrical conductivity, large surface area and low cost. In the recent past years, the electrochemical biosensor

based on nanomaterial, such as metal nanoparticles, carbon nanotubes; metal oxides have been reported [14-15]. To exercise and confirm the functionalities of graphene, much attention has been on the fabrication of graphene nanocomposites as is evidenced by the enhanced sensing platform for the construction of electrochemical sensor and biosensors synergy on the electrocatalytic activity hence advanced sensitivity of sensors. Prussian blue (PB) is an inorganic polycrystalline substance with well-known electrochromic, photophysical, electrocatalytic and magnetic properties [16-18]. In 1978, Neff reported for the first time the successful deposition of Prussian blue on solid electrodes [19-20]. From thereon, enormous number of studies has used different methods for preparation of PB-modified electrodes which have been reported in the literature [20]. The electrochemical stability of Prussian blue film on electrode surfaces have been improved by using different electroactive materials. These materials include screen-printed electrode (SPEs) [21], ordered mesoporous carbon (OMC) [22], polyaniline (PANI), cetyltrimethylammonium bromide (CTAB) [23] and multi-walled carbon nanotubes (MWCNTs) [24]. In this study, we have synthesized and characterized both PB and GO. PB was then deposited on graphene oxide (GO) to increase the stability of the PB film and take advantage of the unique properties of both GO and PB in an attempt to enhance and greatly broaden the application of GO and PB in sensor electrochemistry. The ability of the electrodes to detect hydrogen peroxide in a low potential with different pH ranges in phosphate buffer solution were also studied.

2. EXPERIMENTAL

2.1. Reagents and apparatus

Glassy carbon electrodes (GCE) were purchased from BAS Inc (Tokyo Jaban) natural flake graphite powder, concentrated Sulphuric acid (H_2SO_4), Potassium Permanganate ($KMnO_4$), Hydrogen Peroxide (H_2O_2), Hydrochloric acid (HCl), *N, N*-dimethylformamide (DMF) , Sodium dihydrogen phosphate (NaH_2PO_4), disodium hydrogen phosphate (Na_2HPO_4), potassium hexacyanoferrate ($K_4[Fe(CN)_6].3H_2O$, iron nitrate nonahydrate ($Fe(NO_3)_3.9H_2O$ and alumina oxide (Al_2O_3) were purchased from sigma-Aldrich. All chemicals were of analytical grate and used as received without further purification. All the solutions were prepared with deionized water.

2.2. Electrochemical measurements

Electrochemical measurements were performed using an autolab potentiostat (663 VA stand metrohm Swiss mode). A convectional three-electrode system was employed Ag/AgCl (3M KCl) as a reference electrode, platinum electrode as a counter electrode and glassy carbon electrode (GC) modified with graphene oxide (GO) and Prussian blue (PB) as working electrode for all experiments. A 0.1M phosphate buffer solution (PBS) with different pH solutions were used as an electrolyte solution.

2.3. Synthesis of Prussian blue and graphene oxide

Prussian blue nanoparticles were synthesized as follows: An aqueous solution of $Fe(NO_3)_3.9H_2O$ was added to an aqueous solution of same equal molar mass of $K_4[Fe(CN)_6].3H_2O$. The reaction mixture was vigorously stirred for 10 min. Dark blue precipitate obtained were centrifuged, washed with distilled water three times and with methanol once , and then dried in an oven at 80^{o}C to yield insoluble Prussian blue nanoparticles [25].

Graphene oxide was prepared following the adopted Hummer's method [26]. Summarily, 2 g of natural flake graphite powder was added to 46 ml of cold (0^{o}C) concentrated sulphuric acid (H_2SO_4). Then 6 g of Potassium Permanganate $KMnO_4$ was gradually added with continuous stirring in a cooling ice bath. The mixture was stirred at 35^{o}C for 2 hours. 92 ml of distilled water was slowly added to the mixture and temperature was maintained below 100^{o}C for 15 minutes. After that, 280 ml of Hydrogen Peroxide (H_2O_2) solution was added to the mixture. The product was finally filtered with 500 ml of Hydrochloric acid (HCl) solution to remove metal ions then thoroughly washed with distilled water. Brownish pasty material of GO was obtained.

2.4. Preparation of the modified electrodes

The GCE surface (3 mm in diameter) was cleaned by gentle polishing in aqueous slurry of alumina nanopowder (Sigma-Aldrich) on a mesh paper. The electrode was then subjected to ultrasonic vibration in acetone to remove residual alumina particles that might have been trapped at the surface of the electrode, and then subjected to ultrasonic vibration in deionized water before drying. GC-GO was prepared using 50 mg of graphene oxide (GO) was dispersed in 5 ml of *N,N*-dimethylformamide (DMF) to dissolve in the absence of ultrasonic mixing for 5 min to form a homogeneous solution. About 20 µl drop of GO/DMF solution were dropped on the bare GC electrode and dried in an oven at 50^{o}C for 5 min. the modified electrode is herein denoted as GC-GO. PB film was prepared by sequential deposition method as described by Han *et al* [27]. The GC-Bare or GC-GO electrodes were first immersed in stirred $Fe(NO_3)_3.9H_2O$ solution for 30 min with stirring after which the electrodes were rinsed and dried and then immersed in $K_4[Fe(CN)_6].3H_2O$ solution and stirred for another 30 min, followed by a re-rinsing and a re-drying processes to complete the deposition cycle. The obtained electrodes were described as GC-PB and GC-GO-PB respectively.

2.5. Characterization

Synthesized graphene oxide, Reduced graphene oxide and Prussian blue were characterized by Atomic force microscopy (AFM), Fourier transform infrared (FT-IR), Attenuated total reflectance spectroscopy (ATR), and Field emission scanning electron microscope (FE-SEM). The surface measurements were recorded with a JEOL 7500F Field Emission scanning electron microscope (FE-SEM). Attenuated Total Reflectance (ATR) Fourier Transform infrared (FT-IR) spectra were recorded on a Perkin Elmer Spectrum 100 spectrometer in the 4000-500 region. IR spectra were recorded using Perkin-Elmer Spectrum 400 FT-IR/FT-NIR spectrometer in the range 400 – 4000 cm^{-1}.

3. RESULTS AND DISCUSSION

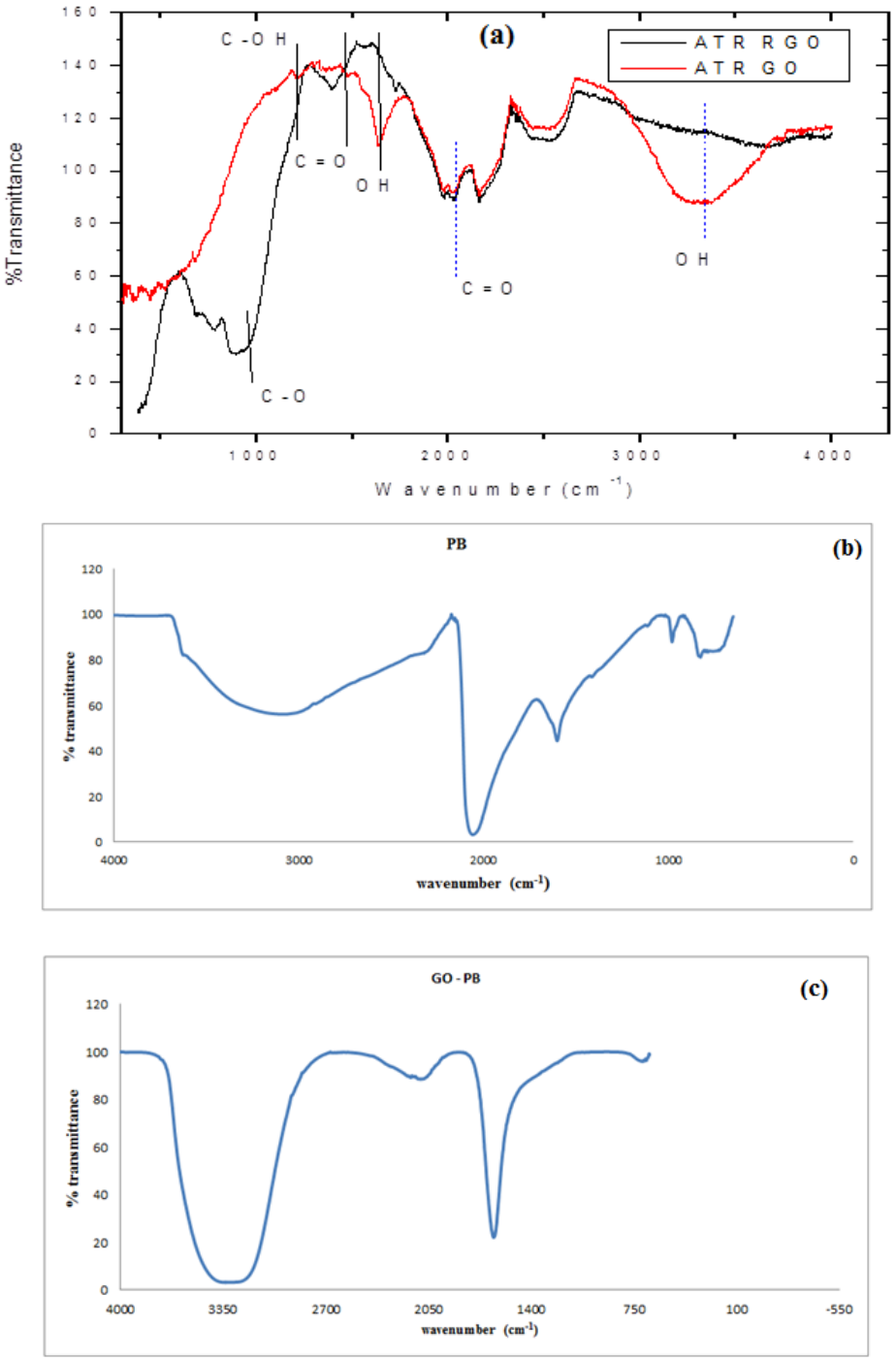

Figure 1. Fourier transforms infrared (FTIR) and Attenuated total reflectance (ATF) Spectra of graphene oxide and reduced graphene oxide (a), Prussian blue nanoparticles (b) and Prussian blue with graphene oxide composite.

Fourier Transform infrared (FTIR), attenuated total reflectance (ATR) spectrum of graphene oxide and reduced graphene oxide is presented in Figure. 1(a). The spectrum shows a peak of reduced graphene oxide representing O-H stretching vibrations observed at 3400 cm^{-1} which was significantly

reduced due to deoxygenation. The C=O at 1720 cm^{-1} in this spectrum is due to the mechanism of exfoliation mainly because of the expansion of CO_2 evolved into the interstices between the graphene sheets during rapid heating, and the C-O stretching vibrations observed at 1060 cm^{-1} is due to the remaining carbonyl groups after the reduction process. The mechanism of exfoliation is mainly the peeling of graphitic structure to pave way for the entering of oxygen during oxidation process. The stretching vibrations at 1220 cm^{-1} and 1060 cm^{-1} on the graphene oxide spectra indicate the presence of C–C skeletal vibrations of the graphite ring. The ATR spectra, figure 1(a), provide evidence that the oxygen-containing functional groups have been removed from graphene oxide. This further confirms the reduction of graphene oxide by chemical reduction method. Figure 1(b) is the FT-IR spectra of Prussian blue nanoparticles, which show several peaks, the strong peak at 2057cm^{-1} which is the characteristic absorption peak of PB is assigned to stretching vibration of C≡N group in potassium hexaferricyanide.

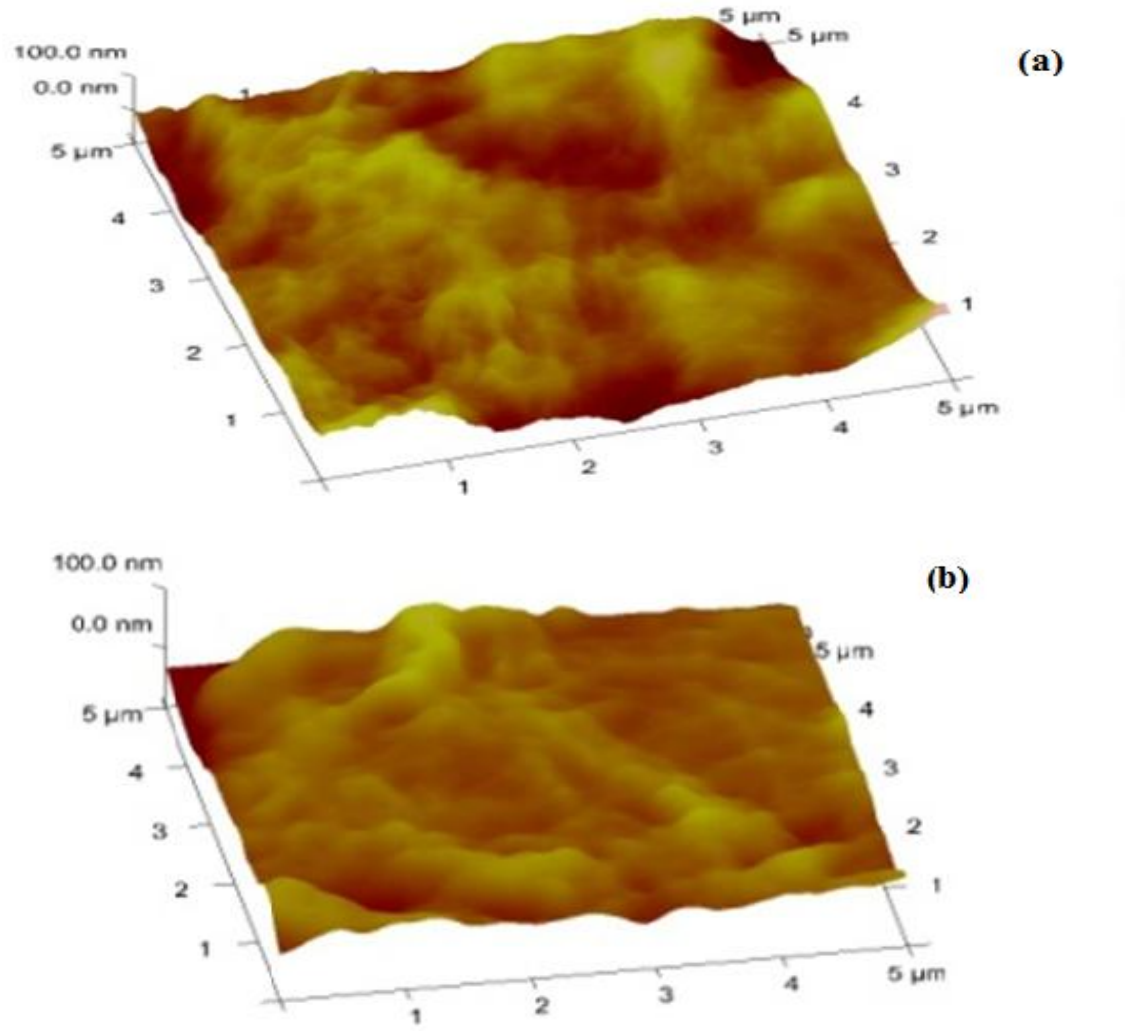

Figure 2. 3D Atomic force microscopy (AFM) topography of (a) graphene oxide and (b) reduced graphene oxide.

The absorption bands near 3215 and 1602 cm^{-1} is assigned to the O–H stretching mode and H–O–H bending mode respectively, which indicate the existence of interstitial forces of attraction in the sample. The FTIR spectra of the GO-PB composite, figure 1(c), show new absorptions bands formed due to the combination of GO-PB. The strong peak in the PB spectra observed at 2057cm^{-1} is reduced and shifted to 2099cm^{-1} which indicates the C≡N stretching absorption band in the Fe^{2+}-CN-Fe^{3+} of PB.

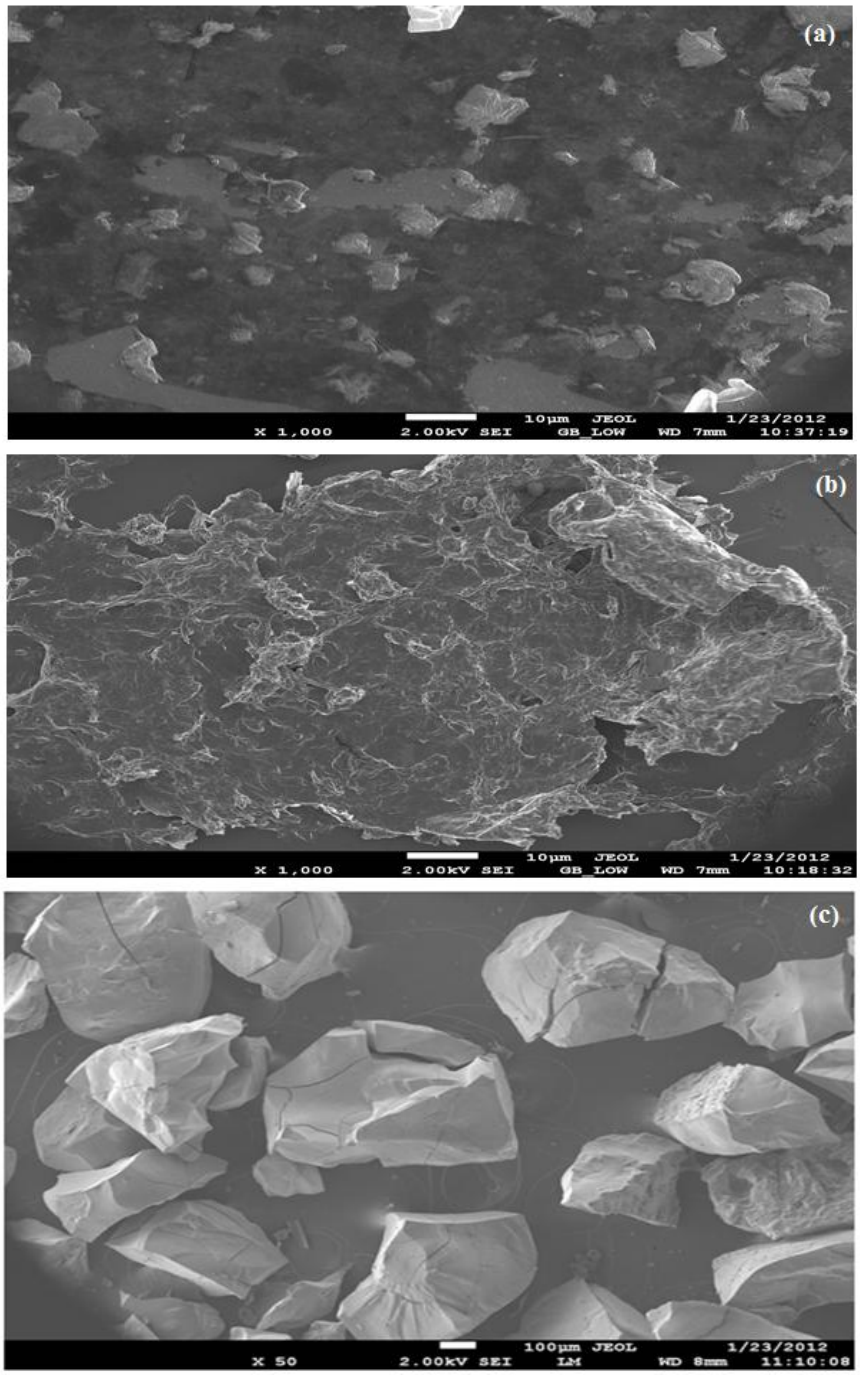

Figure 3. Scanning electron microscopy (SEM) images of (a) graphene oxide (b) Reduced graphene oxide and (c) Prussian blue nanoparticles.

The level of exfoliation was evaluated by atomic force microscopy (AFM) as presented in Figure 2 (a & b). The AFM images show a three dimensional AFM topography of graphene oxide and reduced graphene respectively. The GO sheets are expected to be thicker due to the presence of covalently bonded oxygen and the displacement of sp^3 hybridized carbon atoms slightly above and below the original graphene plane. The height difference between rows is 1 nm in GO and 1.2 nm in RGO indicating a single graphene oxide sheet due to intercalating of oxygen into the graphite gallery. The results reveal graphene oxide and reduced graphene oxide were obtained in the synthesis.

The scanning electron micrograph (SEM) of the morphology of graphene oxide, reduced graphene oxide and Prussian blue nanoparticles are presented in figure 3 (a to c). According to literature reports [28-29], the chemical conversion of graphite oxide to graphene, produce holes and defects on the carbon grid. It is possible that these holes are a result of the removal of oxygen functional group during the reduction process. It is also possible that the nanocomposites can grow around these holes and defects and are inclined to insert into graphene sheets [30]. In addition, the rigid particles may also easily sink into the supported materials [31]. By visual inspection, it can be seen that the GO image looks lighter while the RGO image looks darker. This could be attributed to the fact that as the oxygen functional groups are removed during reduction process, the separated GO sheets during intercalation now stick together and result in a decrease in interlayer spacing of single sheets. This further confirms the reduction of GO into RGO. In figure 4 (c) scanning electron microscopy (SEM) was used to determine the particle size and distribution of the Prussian blue nanoparticles synthesized. The image show the PB as aggregates of nanoparticles of high dimension with no precise shape.

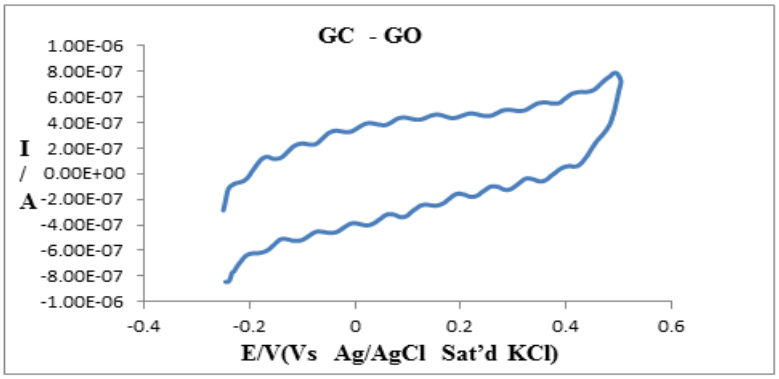

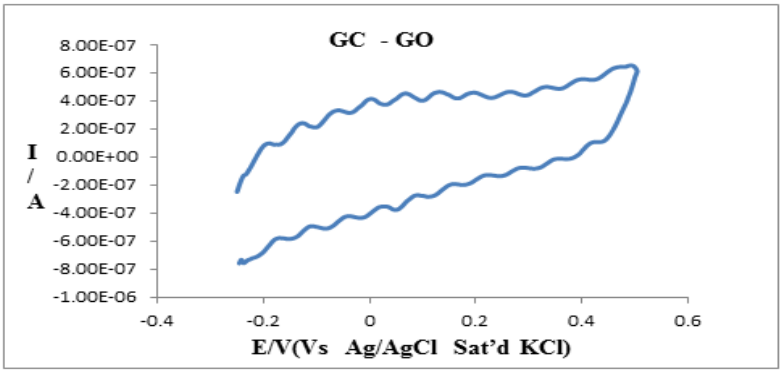

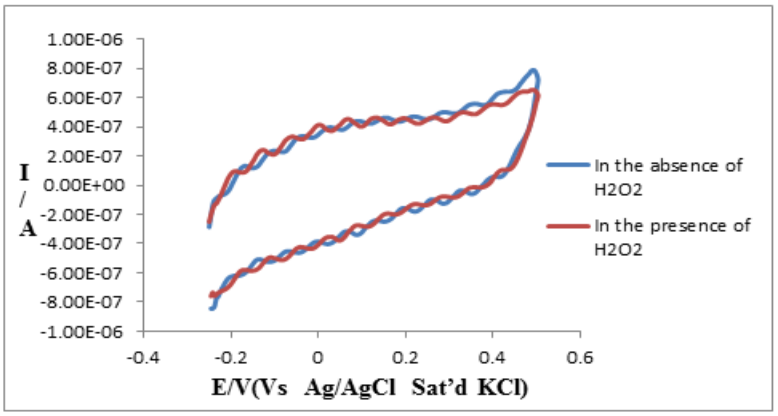

Figure 4. Cyclic voltammograms of GC-GO electrode (a)before and (b) after injection of 25µl H_2O_2 in 0.1M PBS pH 7.4 (c) overlay of the cyclic voltamograms of (a) and (b).

The electrochemical properties of GC-GO, GC-PB and GC-GO-PB electrodes were studied in 0.1 M phosphate buffer solution at different pH values, using cyclic voltammetry recorded between -250 to 500mV at scan rate of 100mV/s. The cyclic voltammograms of glassy carbon electrode modified graphene oxide (GC-GO) in the absence and presence of hydrogen peroxide in 0.1 M phosphate buffer solution at pH 7.4 is presented in figure 4 (a & b). The overlay of the electrode response in the absence and presence of hydrogen peroxide is presented in figure 4 (c). The overlay of the electrode response in the presence and absence of hydrogen peroxide show no response observed. This gives the indication that graphene oxide (GO) modified GC electrode does not detect hydrogen peroxide at the potential measured.

Cyclic voltammograms of Prussian blue modified glassy carbon electrode (GC-PB) in the absence and presence of hydrogen peroxide in 0.1 M phosphate buffer solution at pH 3, pH 5.12 and pH 7.4 are presented in figure 5.

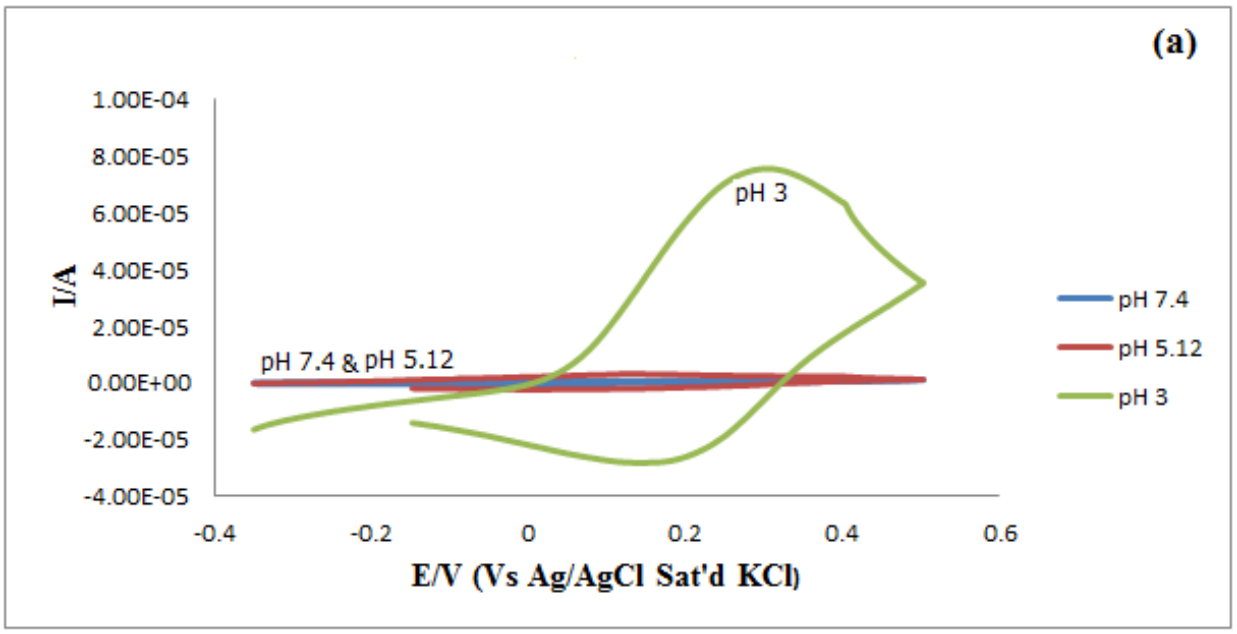

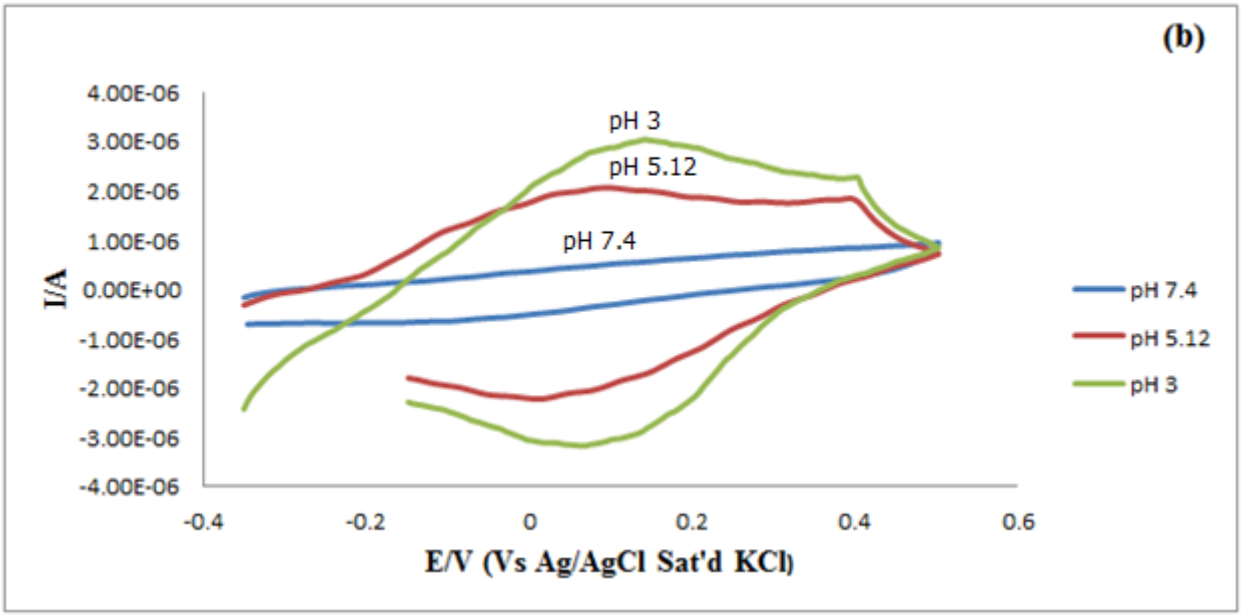

Figure 5. Cyclic voltammograms of GC-PB electrode (a) before and (b) after injection of 25µl H_2O_2 in 0.1M PBS at different pH values.

It is well known that Prussian blue has certain intrinsic peroxidase activity due to its close similarity with peroxidase, thus it can be engaged to catalyze the reduction of hydrogen peroxide [23]. The GC-PB electrode in the absence of hydrogen peroxide, figure 5 (a) does not show any electrochemical response at pH 5.12 and pH 7.4, while at pH 3 anodic and cathodic responses are observed. In the presence of hydrogen peroxide, figure 5 (b), anodic and cathodic responses are observed. The highest response is at pH 5.12 while the lowest response is observed at pH 7.4. The high response at pH 5.12 is due to the fact that at high pH, Prussian blue loses its stability. GC-PB electrode is observed to detect the presence of hydrogen peroxide at pH 5.12 and slightly at pH 7.4. At pH 3, in both voltammograms, a high response was observed indicating the GC-PB electrode at pH 3 did not react both in the presence or absence of hydrogen peroxide.

The cyclic voltammograms of GC-GO-PB electrode in the absence or presence of hydrogen peroxide in 0.1 M phosphate buffer solution at pH 3, pH 5.12 and pH 7.4 are presented in figure 6. In the absence of hydrogen peroxide, figure 6 (a), anodic responses are observed at all pH values. The highest response is observed at pH 7.4 and the lowest in acidic medium at pH 3. The cathodic response on the other hand is more pronounced at pH 5.12. In the presence of hydrogen peroxide, figure 6 (b), the GC-GO-PB electrode produces both anodic and cathodic responses. Two anodic and cathodic peaks are observed at pH 7.4 indicating two electron transfer reactions taking place. At pH 5.12, the electrode reaction fizzled away showing that the presence of hydrogen peroxide has adversely affected the anodic response previously observed. These results indicate the presence of graphene oxide has considerably enhanced the electrochemical stability of PB film and its detection of hydrogen peroxide. The cyclic voltammograms of GC-PB and GC-GO-PB electrode reactions observed could be explained as a one electron transfer reaction in neutral or slightly acidic medium. For the GC-GO-PB electrode,

this is a conversion of a sp^2 to sp^3 bond in graphene. For the GC-PB electrode, the electrochemical stability of Prussian blue nanoparticles could be due to the –CN groups of PB.

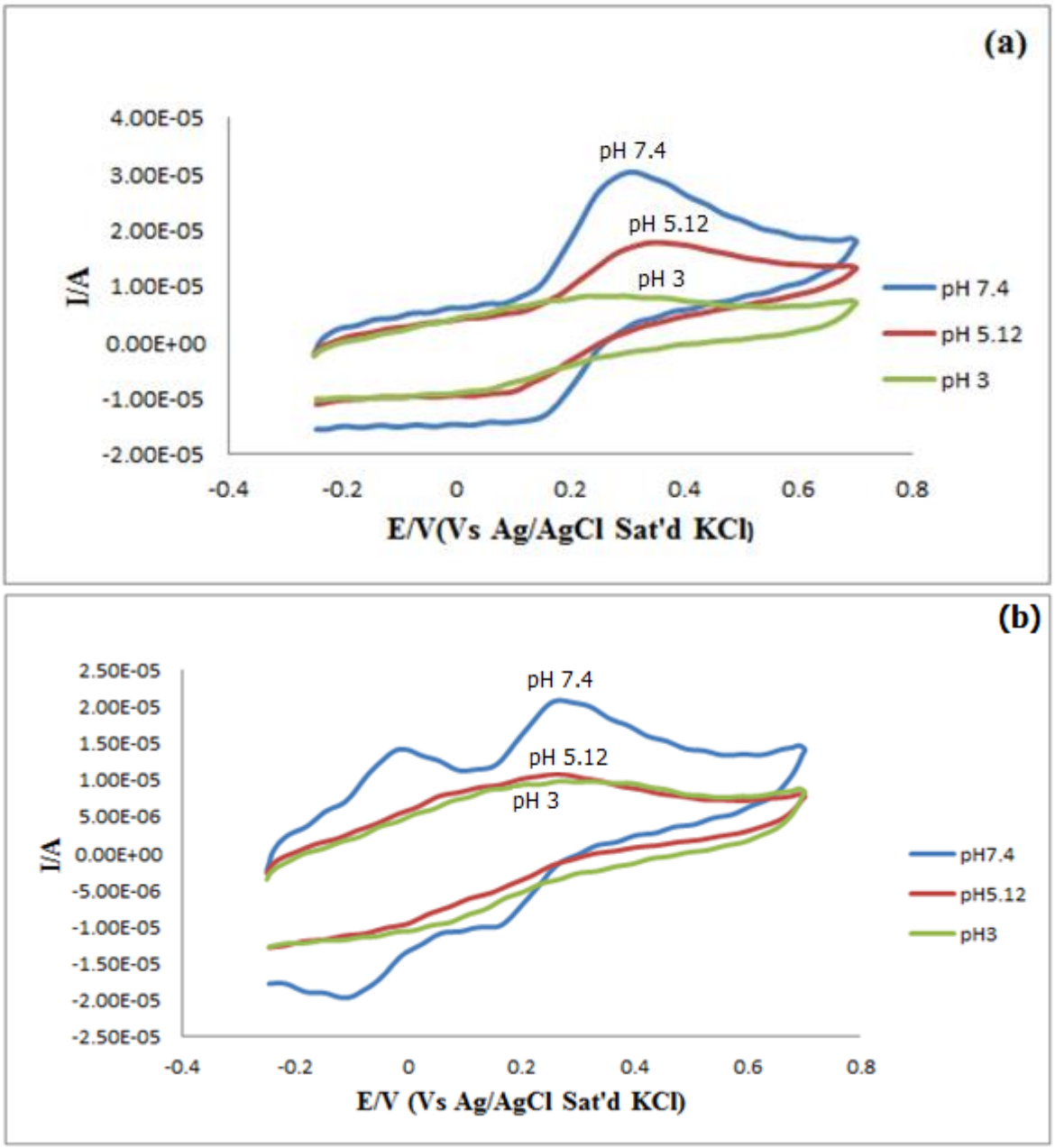

Figure 6. Cyclic voltammograms of GC-GO-PB electrode (a) before and (b) after injection of 25 µl H_2O_2 in 0.1M PBS at different pH values.

The electrochemical properties of GC-GO, GC-PB and GC-GO-PB electrodes were studied in 0.1 M phosphate buffer solution at different pH values, using square wave voltammetry recorded between -700 mV to 700 mV at scan rate of 50 mV/s. The square wave voltammograms of glassy carbon electrode modified graphene oxide (GC-GO) before and after injected of H_2O_2 in 0.1 M phosphate buffer solution at pH 7.4 is presented in figure 7 (a & b). Their overlay is presented in figure

7 (c). These results are in agreement with cyclic voltammogram results presented in figure 4, for GC-GO, in which no responses were observed both in the absence and presence of hydrogen peroxide.

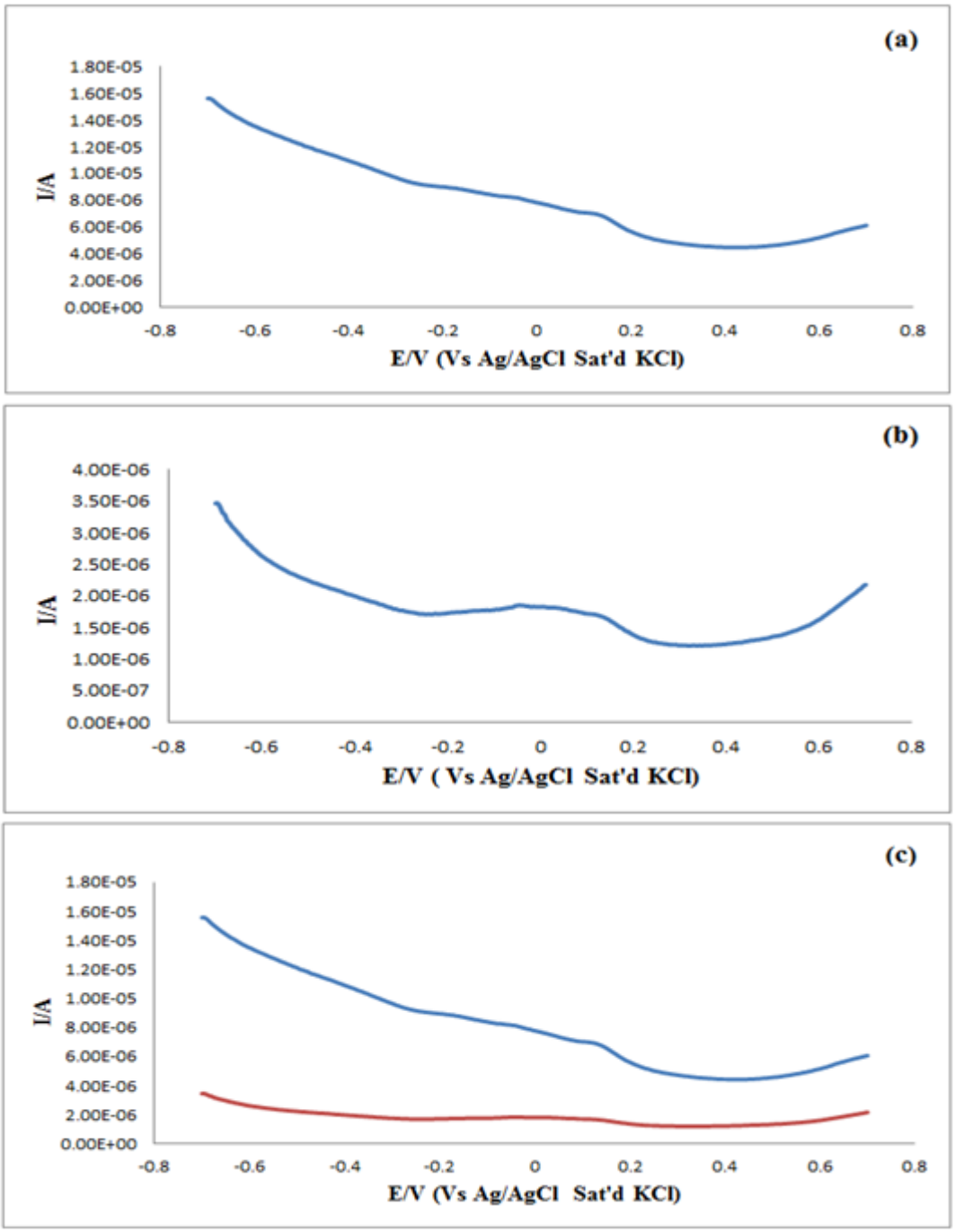

Figure 7. Square wave voltammograms of GC-GO electrode (a) before and (b) after injection of 25 µl H_2O_2 in 0.1M PBS pH 7.4 (c) overlay of a and b.

Square wave voltammetry of Prussian blue modified glassy carbon electrode (GC-PB) before and after injection of H_2O_2 in 0.1 M PBS at pH 3, pH 5.12 and pH 7.4 are presented in figure 8 (a & b). The GC-PB electrode in the absence of hydrogen peroxide, figure 8 (a) does not show any significant

electrochemical response at pH 5.12 and pH 7.4, while at pH 3 a high anodic responses is observed. The high response current at pH 3, is observed around 0.12V while at pH 5.12 and pH 7.4 no responses were observed at 0.03 and -0.06V respectively. In the presence of hydrogen peroxide, figure 8 (b), anodic response are observed at pH 3 giving rise to a small shoulder peak.

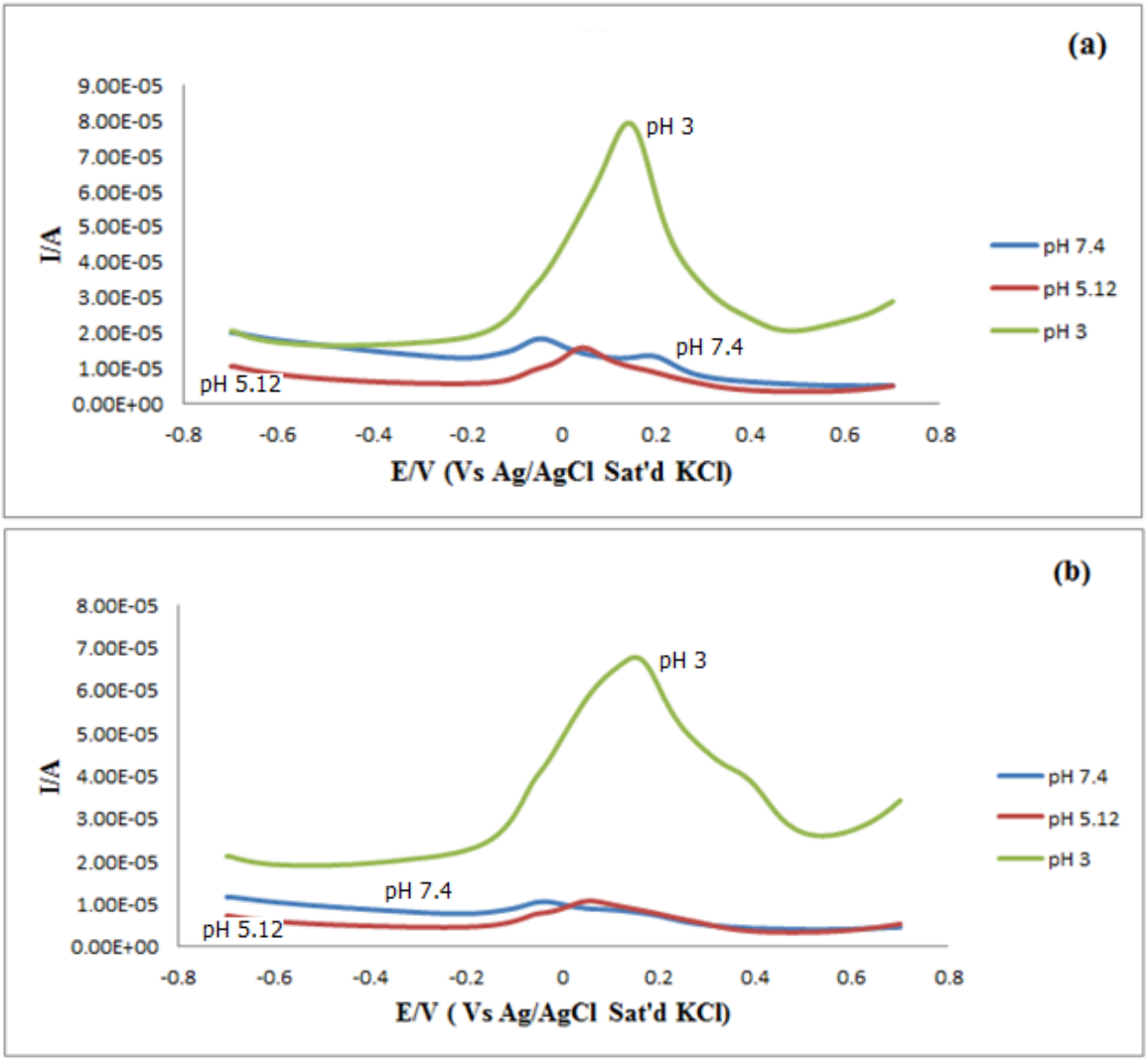

Figure 8. Square wave voltammograms of GC-PB electrode (a) before and (b) after injection of 25 µl H_2O_2 in 0.1M PBS at different pH values.

Square wave voltammetry of GC-GO-PB before and after injection of H_2O_2 in 0.1 M PBS at pH 3, pH 5.12 and pH 7.4 are presented in figure 9 (a & b). In the absence of hydrogen peroxide, figure 9 (a), anodic and cathodic current responses are observed. The highest anodic response is observed at pH 7.4, while at pH 3 and 5.12, low anodic responses are observed respectively. At pH 5.12, a small but significant cathodic response is observed at a potential of 0.6 V. In the presence of hydrogen peroxide, figure 9 (b), the GC-GO-PB electrode again produces both anodic and cathodic responses. No change in response is observed at pH 7.4 which again records a high current response

with a peak at about -0.1 V. Two anodic peaks at 0.15 V and 0.4 V are observed at pH 3. The cathodic peak with a voltage of 0.5 V at pH 5.12 is seen to have increased.

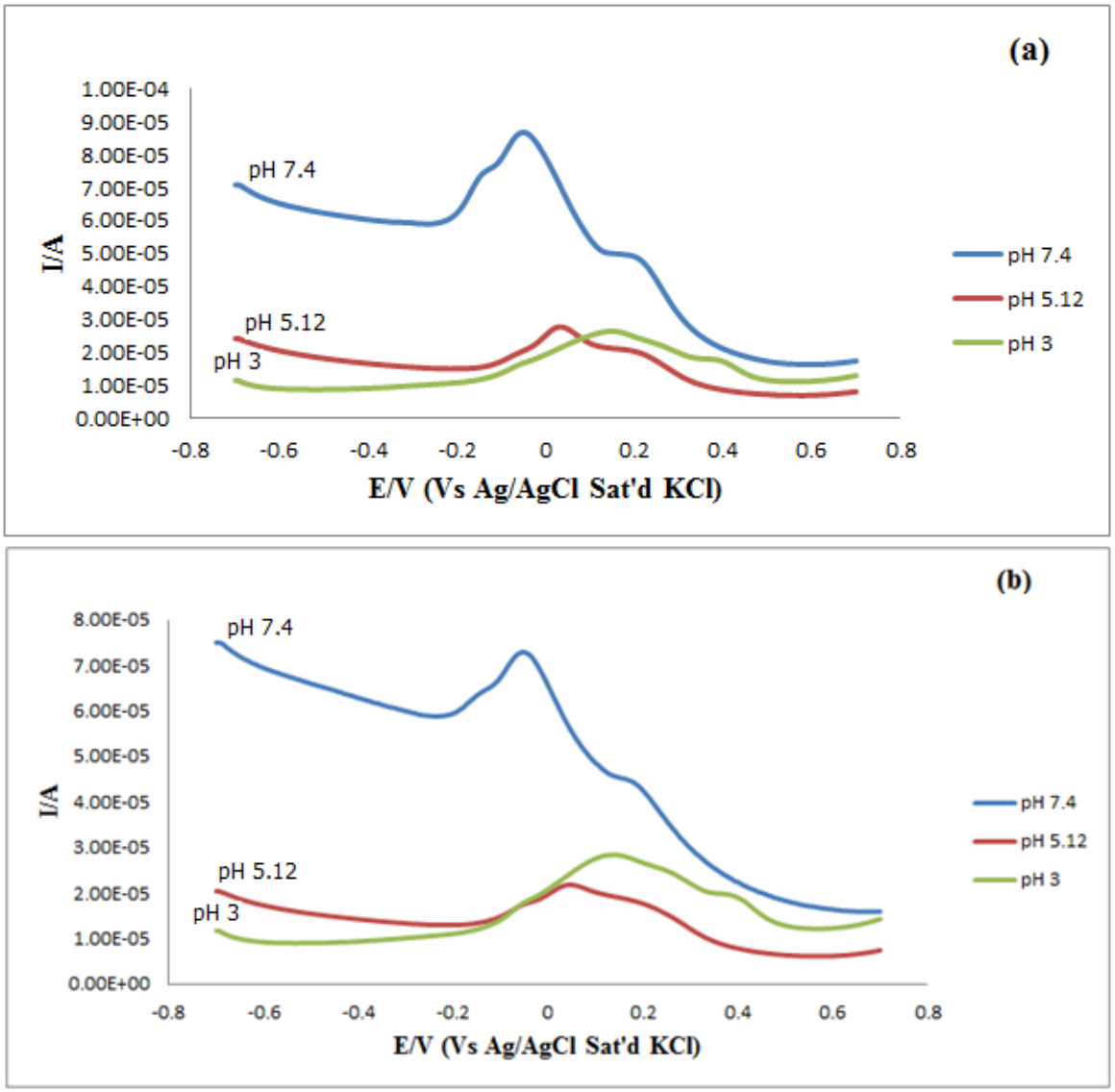

Figure 9. Square wave voltammograms of GC-GO-PB electrode (a) before and (b) after injection of 25µl H_2O_2 in 0.1M PBS at different pH values.

The optimum response pH in the square wave voltammetry of GC-GO-PB electrode is pH 3. There is similarity in the sensitivity response for the cyclic and square wave voltammograms for the GC-PB and GC-GO-PB electrodes.

4. CONCLUSION

Prussian blue and graphene oxide were synthesized used in the modification of glass carbon electrodes for the chemical detection of hydrogen peroxide. Cyclic and square wave voltammetry of

GC-PB and GC-GO-PB electrodes show significant detection of hydrogen peroxide predominantly at pH 5.12 and 7.4 for the GC-PB electrode. For the GC-GO-PB electrode, current responses indicating the detection of hydrogen peroxide were observed at all pH values for the cyclic and square wave voltammetry. The most significant detection of hydrogen peroxide on the GC-GO-PB electrode was found at pH 7.4 in the cyclic voltammetry and at pH 5.12 in the square wave voltammetry.

ACKNOWLEDGMENTS
This work was supported by a research grant from the faculty of applied and computer science research and publications committee of Vaal University of Technology, Vanderbijlpark.

References

1. A. K. Geim, K. S. Novoselov, *Nat. Mater*. 6 (2007) 183-191.
2. X.W. Liu, Z.J. Yao, Y.F. Wang, X.W. Wei, *Colloids. Surf. B: Biointerfaces*. 18(2010) 508-512.
3. Y. Shao, J. Wang, H. Wu, J. Liu, I.A. Aksay, Y. Lin, *Electroanalysis,* 22,10 (2010) 1027-1036.
4. Y. Zhang, X. Sun, L. Zhu, H. Shen, N. Jia, *Electrochimica Acta* 56 (2011) 1239-1245.
5. L. Feng, Y. Chen, J. Ren, X, Qu, *Biomaterials* 32 (2011) 2930-2937.
6. X. Wang, L. Zhi, K. Mullen, *Nano Lett*, 8, 1 (2008) 323-327.
7. W. Wu, Z. Liu, L. A. Jauregui, Q. Yu, R. Pillai, H. Cao, J. Bao, Y. P. Chen, S-S Pei, *Sens. Actuators* B 150 (2010) 296-300.
8. A.V. Rozhkov, G. Giavaras, Y. P. Bliokh, V. Freilikher, F. Nori, *Physics Reports* 503 (2011) 77-114.
9. V.K. Singh, M. Patra, M. Manoth, G.S. Gowd, S.R. Vadera, N. Kumar, *New Carbon Mater.* 24(2) (2009) 147-152.
10. A. Castellanos-Gomez, R.H.M. Smit, N. Agrait, G. Rubio-Bollinger, *Carbon* 50 (2011), 932 – 938.
11. P.C. Divari, G.S. Kliros, *Physics E* 42 (2010) 2431-2435.
12. T.S. Sreeprasad, S.M. Maliyekkal, K.P. Lisha, T. Pradeep, *J. Hazard. Mater.* 186 (2011) 921-931.
13. C. Zhang, W. W Tjiu, W. Fan, Z. Yang, S. Huanga, T. Liu, *J. Mater. Chem*. 21 (2011) 18011.
14. E. Jin, X. Lu, L. Cui, D. Chao, C. Wang, *Electrchemica Acta* 55 (2010) 7230-7234.
15. T. Kuila, S. Bose, P. Khanra, A. K. Mishra, N. H. Kim, J. H. Lee, *Biosens. Bioelectron* 26 (2011) 4637-4648.
16. Z. Li. J. Chen, W. Li, K. Chen, L. Nie, S.Yao, *J. Electroanal. Chem*. 603 (2007) 59-66.
17. J. Zhang, J. Li, F. Yang, B. Zhang, X. Yang, *Sens. Actuators*. B143 (2009) 373-380.
18. Y. Zhang, Y. Wen, Y. Liu, D. Li, J. Li, *Electrochem. Commun*. 6 (2004) 1180-1184.
19. F. Ricci, G. Palleshci, *Biosens. Bioelectron*. 21, (2005) 389-407.
20. L. Lin, X. Huang, L. Wang, A. Tang, *Solid State Science*. 12 (2010) 1764-1769.
21. F. Ricci, A. Amine, G. Palleschi, D.J. Moscone, *Biosens. Bioelectron*. 18 (2003) 165-174.
22. J. Bai, B. Qi, J.C. Ndamanisha, L.P Guo, *Micropor. Mesopor. Mater*. 119 (2009) 193-199.
23. R. Vittal, K.J. Kim, H. Gomathi, V. Yegnaraman, *J. Phys. Chem*. B112 (2008) 1149-1156.
24. N. Zhang, G. Wang, A. Gu, Y. Feng, B. Fang, *Mirochim. Acta.* 168 (2010) 129-134.
25. A. Gotoh, H. Uchida, M. Ishizaki, T. Satoh, S. Kage, S. Okamoto, M. Ohta, M. Sakamoto, T. Kawamoto, H. Tanaka, M. Tokumoto, S. Hara, H. Shiozaki, M. Yamada, M. Miyake, M. Kurihara, *J. Nanotechnology*. 18 (2007) 345-609
26. W.S. Hummers, R. E. Offenman, *J. Am. Chem. Soc*. 80 (1958) 1339.
27. S. Han, Y. Chen, R. Pang, P. Wan, *Ind. Eng. Chem. Res*. 2007, 46, 6847-6851.
28. K. N. Kudin, B. Ozbas, H. C. Schniepp, R. K. Prud'homme, I. A. Aksay, R Car, *Nano. Lett*. 8 (2008) 36-41.

29. M. J. McAllister, J. L. Li, D. H. Adamson, H. C. Schniepp, A. A. Abdala, J. Liu, M. Herrera-Alonso, D. L. Milius, R. Car, I. A. Aksay, *Chem. Mater*. 19 (2007) 4396-4404.
30. Y. Yu, L. L. Ma, W. Y. Huang, F. P. Du, J. C. Yu, J. G. Yu, *Carbon*, 43,34 (2005) 670-673.
31. S. Pan, X. Liu, X. Wang, *Mater. Charact.* 62 (11) (2011) 1094-1101.